Full Paper

Propellants, Explosives, Pyrotechnics

doi.org/10.1002/prep.202100071

Shock Initiation Investigation of a Pressed Trinitrotoluene Explosive

Lixiaosong Du,[a] Shaohua Jin,[a] Zhiyue Liu,[b] Lijie Li,[a] Mengxia Wang,[a] Pengsong Nie,[a] and Junfeng Wang*[b]

Abstract: The shock initiation process of a pressed trinitrotoluene (TNT) at density of 1.563 g cm^{-3} was studied by manganese-copper gauge measurement experiments as well as numerical simulation for assessing the performance and detonation growth characteristics in such pressed samples. Through gap test, the shock pressure histories at different inner positions of the target TNT charges were measured. The parameterization on shock initiation model proposed by Lee & Tarver for numerical simulation were accomplished. The equation of state for unreacted explosive in the model was obtained by fitting Hugoniot data calculated from molecular dynamic simulation and shock temperature based on Walsh's solution. The equation of state for the detonation products was theoretically predicted by EXPLO5. Combining those procedures, the ignition and growth model for a pressed TNT was accurately parameterized together with experimental pressure history data. Experiment and simulation indicate that when the input pressures are 6.13 GPa and 8.67 GPa, respectively, the corresponding run distances to detonation are >9 mm and 6 mm. The calculated pressure growth histories at different inner positions of the pressed TNT sample can well reproduce the correspondingly measured values. The determined ignition and growth model will be expected to put in use in subsequent simulation analysis with complex geometrical scenarios.

Keywords: Pressed trinitrotoluene (TNT) · Gap test · Ignition and Growth model · Run distance to detonation

1 Introduction

The safety performances of solid non-homogeneous explosives under shock loading have increasingly been urgent in recent years due to the possibly unexpected explosion accident. Trinitrotoluene (TNT) [1] is a widely used explosive in various applications, so it is necessary to pay more attention on its safe usage. Although previous studies [2–5] explored shock-to-detonation transition and decomposition data of TNT in casted and pressed states, the theoretical models were simple and insufficient. Tarver [2] conducted several gap tests and parameterized a binomial Ignition and Growth (IG) model for casted TNT. However, up to now, a reliable theoretical shock-initiation model for pressed TNT has not been presented publicly elsewhere.

Based on this fact, we established a gap test assembly to observe the shock-to-detonation progress in pressed TNT (1.563 g cm^{-3}) in the light of the ordinary gap test modification [6]. The pressure growth histories measuring from the shock input end were obtained via taking use of manganin pressure gauge [7] embedded in the pressed TNT sample. The JWL equations of state for both unreacted explosives and detonation products being required for numerical simulation were fitted from shock Hugoniot and isentropic expansion data predicted by theoretical methods [8–11]. Combined with the currently measured pressure histories, the parameterization of the Ignition and Growth model [12] had been accomplished. It became possible to quantitatively determine the run distance to detonation for such pressed density TNT. Furthermore, the shock initiation properties of TNT with different densities was also presented for discussion.

2 Experimental Section

2.1 Experiment

As shown in Figures 1 and 2, the gap test apparatus was used for measuring shock pressure histories at different positions in the target TNT charge via manganin gages after detonation of main charge. This setup was able to explore the detailed initiation process of pressed TNT accompanying shock-to-detonation phenomenon.

In the experiment system, a plane wave generator was used to cause initiation of main charge in rather flat form. A

[a] *L. Du, S. Jin, L. Li, M. Wang, P. Nie*
School of Materials Science and Engineering, Beijing Institute of Technology, Zhongguancun South Street 5, Beijing 100081, China
[b] *Z. Liu, J. Wang*
State Key Laboratory of Explosion Science, Beijing Institute of Technology, Zhongguancun South Street 5, Beijing 100081, China
**e-mail: wjf2015@bit.edu.cn*

Supporting information for this article is available on the WWW under https://doi.org/10.1002/prep.202100071

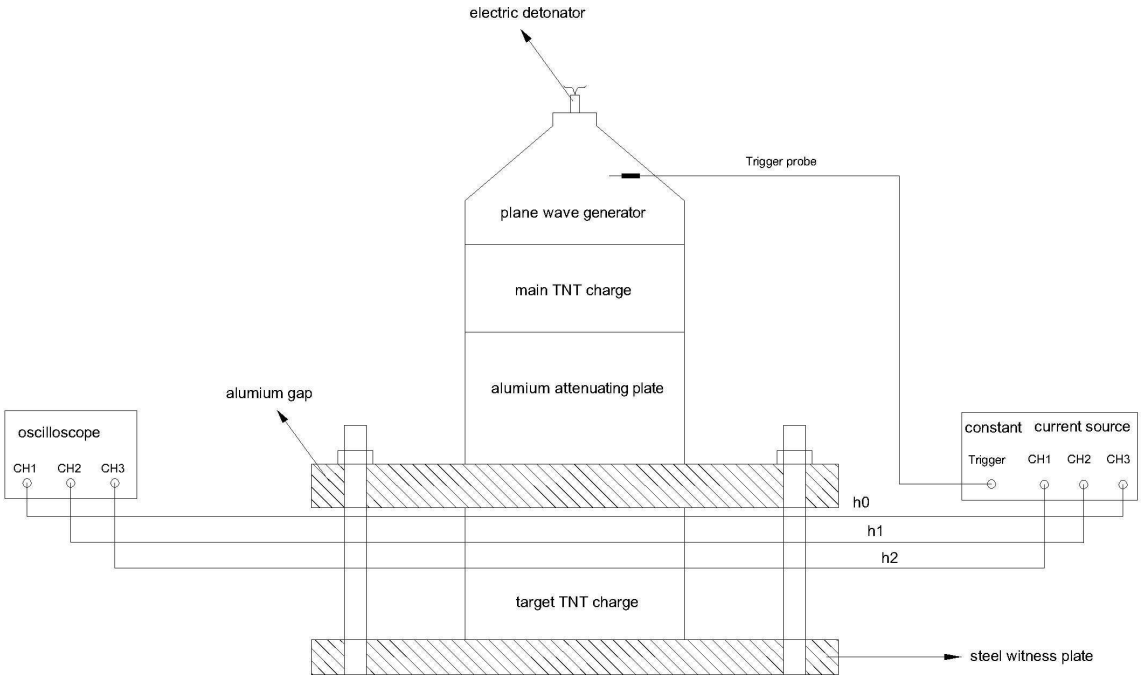

Figure 1. Diagram of gap test.

Figure 2. Snapshot of the actual test setup.

trigger probe was attached on the side of plane wave generator for the start of pressure measuring system. When shock wave passed by the different positions in the target TNT charge, the oscilloscope recorded the voltage signals originated from pre-embedded manganin gages at the corresponding positions. The voltage signals were then converted into the pressure-time curves for the purpose of modelling and analysis. The detailed positions for manganin gages and the thicknesses of the attenuation plate were listed in Table 1.

Table 1. The detailed experimental design setups.

Shot No.	Thickness of aluminium plate	Positions of manganin gauge in target TNT
1	40 mm	0 mm
		6 mm
2	50 mm	0 mm
		3 mm
		9 mm

2.2 Simulation

The whole process was simulated by a finite element method through numerically solving the governing conservation equations. The reactive process of explosive after shock action was described by the model proposed by Lee-Tarver. The model was generally called Ignition and Growth (IG) model and had successfully been applied to shock initiation of solid explosives. The IG model is of the following form [12],

$$\frac{\partial F}{\partial t} = \underbrace{I(1-F)^b\left(\frac{\rho}{\rho_0}-1-a\right)^x}_{0<F<F_{igmax}} + \underbrace{G_1(1-F)^c F^d P^y}_{0<F<F_{slowmax}} + \underbrace{G_2(1-F)^e F^g P^z}_{F_{fastmin}<F<1} \quad (1)$$

$$P_s = A_s e^{-R_{1s}V_{rs}} + B_s e^{-R_{2s}V_{rs}} + \frac{w_s C v_s T_s}{V_{rs}} \quad (2)$$

$$P_g = A_g e^{-R_{1g}V_{rg}} + B_g e^{-R_{2g}V_{rg}} + \frac{w_g C v_g T_g}{V_{rg}} \quad (3)$$

where: F is the mass reaction fraction of explosive, $=0$ meaning unreacted, $=1$ being complete reaction; P is pressure; T is temperature; ρ is current density; ρ_0 is initial density; I, a, b, c, d, e, g, x, y and z are fitting constants for specific explosive; F_{igmax} is top limit of the explosive mass fraction for ignition phase, $F_{slowmax}$ and $F_{fastmin}$ are upper and lower cutoff values of the mass fraction for slow and fast deflagration phases, respectively; Subscripts s and g indicate the unreacted explosive and detonation products; V_r is relative specific volume; C_v is specific heat capacity under constant volume condition; A, B, R_1, R_2 and ω are fitting constants.

However, the parameters in IG model and equations of states (EOS) must be determined for specific explosive. Based on our understanding toward this subject, we established our own treatment to obtain those parameters, especially for the unreacted and products equations of state. For unreacted phase equation of state, the shock velocity and particle velocity form was adopted, and their relation was gained by molecular dynamics method [8–9]. In the following, the temperature in unreacted phase was predicted by Walsh method [10]. After obtaining those data, the JWL form EOS would be gained, expressed by Eq. (2). For the products, EXPLO5 [11] was applied to give isentropic expansion data, which is fitting into the form of Eq. (3). The parameters in reactive rate equation of the Ignition and Growth model were determined by matching numerical simulation results into the experimentally measured pressure histories. The detailed molecular dynamic method, shock temperature calculation, IG parameterization approach and numerical modelling procedures were presented in the *Supplementary Materials*.

3 Results and Discussion

3.1 Experimental Pressure Histories

For the established gap test assembly in Figures 1 and 2, the measured pressure history curves were shown in Figure 3 for the pressed TNT with density of 1.563 g cm^{-3}.

The curves in Figure 3(1) were the results of the Shot No.1 (see Table 1). The pressure gage at 0 mm position exhibited relatively flat variation history, meaning that the explosive was simply compressed with no decomposition. However, the gage at 6 mm location presented fast rise in

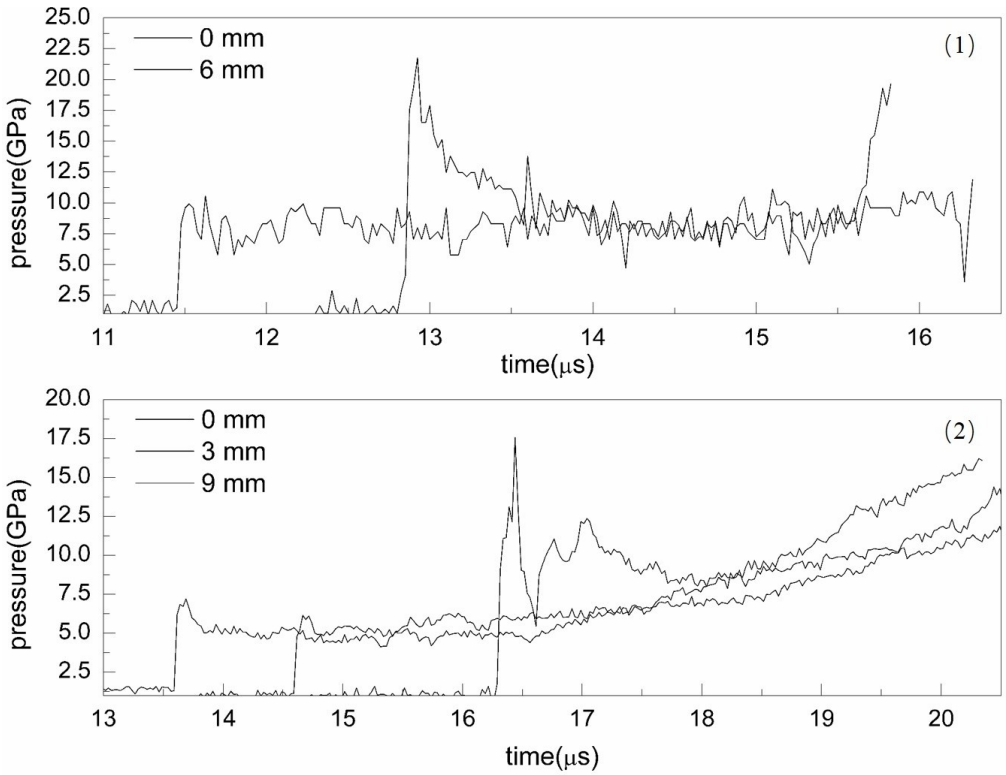

Figure 3. The measured pressure histories in gap test experiments as manganin gages embedding at different locations of target pressed TNT charge; (1) for Shot No.1 and (2) for Shot No. 2.

pressure with big value equivalent to the Chapman-Jouguel (CJ) pressure of the TNT. It meant that at that location the current pressed TNT was initiated to detonation completely. Furthermore, for Shot No.2 test, the pressures histories (Figure 3(2)) of three locations (0 mm, 3 mm and 9 mm) were recorded by embedding the manganin gages there, respectively. Within the range of 0 to 3 mm locations, the amplitude of shock pressure was not observed with any change. It meant that little reaction is initiated locally. After shock wave arriving at 9 mm distance, it was obviously pressure rise owing to shock initiated reaction.

From the tests, we also obtained the run distance to detonation data for the pressed TNT approximately, together with those data from casted TNT [2], listing in Table 2 for comparison. For a given shock pressure input, we noticed that the pressed TNT undergone a shorter initiation distance to detonation than casted TNT. That meant the pressed TNT was more sensitive than casted TNT under shock loading. Belinets [4] reported the phenomenon that the decomposition rate in pressed TNT (1.56 g cm^{-3}) was 5–7 times higher than in casted TNT (1.61 g cm^{-3}) [5] at the pressure between 2–4 GPa up to the detonation level. Campbell's works [13] also indicating that the pressed TNT with lower density behave shorter time of run to detonation, thus more sensitive to shock wave.

The existence of the difference on shock initiation between pressed and casted TNT at nearly similar packing density was due to that the pressed TNT may be of more tiny defects inside the sample than ordinary casted TNT. Pressed TNT was manufactured simply by compressing the flake-like TNT particulate into a column. Rather, casted TNT was gained from the melting phase. Comparatively, under shock loading, pressed TNT was more probable to cause high temperature locations corresponding to the positions with tiny defects inside. The high temperature locations brought out the fast chemical decomposition to form ignition source for the surrounding matters, then, the chemical reaction rapidly spread across the whole explosive column. As a result, pressed TNT had a shorter distance to detonation phase after ignition and growth states. From view of the sensitiveness, the pressed TNT is of being more sensitivity to shock wave than that of casted TNT.

Table 2. Data of the run distance to detonation for pressed and cast TNT.

	ρ_0 (g cm^{-3})	Input pressure (GPa)	L (mm)
Pressed TNT	1.563	6.13	>9
		8.67	6
	1.56	4	>16[a]
Casted TNT	1.61	6.5	12[a]
		8.5	>15[a]

Note: Superscript a in Table indicates data from Figures 4, 7 and 11 in Reference [2].

3.2 Parameters in Ignition and Growth Model

For current pressed TNT, we obtained the relevant parameters in IG model by establishing modelling framework. The shock velocity and particle velocity data for pressed TNT were gained by molecular dynamics simulation. The corresponding result for the particle velocities (U_p) and loading shock velocities (U_s) were summarized in Table 3. In order to check the accuracy of molecular dynamics calculation, we further calculated the similar Hugoniot data of TNT with density of 1.635 g cm^{-3} by molecular simulation, then, the results were compared with the corresponding experimental data from Reference [14]. At the same time, we also collected experimental Hugoniot data for several density TNT and plotted them together with those from our pressed TNT for analysis. Those figures were presented in Figures 4(1)–(2).

From Figure 4(1), the molecular dynamics simulation may give satisfactory result by comparing the calculated data with experimental ones for 1.635 g cm^{-3} TNT. The consistency provided us some belief on the acquirement of Hugoniot data for other densities of TNT by such simulation technique. From Figure 4(2), through comparing Hugoniot data from molecular simulation for the current pressed TNT with the available experimental data of greater and lower densities TNT, the results lay between them. It is consistent with the common understanding for this issue.

Based on U_s-U_p data of pressed TNT, we calculated pressures, specific volumes and temperatures along its Hugoniot line. Then, substituting this set of data into Eq. (2) reached the acquirement of parameters for unreacted explosive. On the other hand, the parameters for detonation products were evaluated by the EXPLO5 code. All those results were given in Table 4. Finally, the parameterization of reaction rate equation (Eq. (1)) was done through numerical simulation by matching the computed pressures with measured pressure history. Those calibrated parameters in IG model for the pressed TNT were shown in Table 5.

Figure 5 presents the experimentally measured pressure profiles and the corresponding simulated pressure curves.

As seen in Figure 5(1), the initial input shock pressure in Shot No.1 was of 8.67 GPa. After shock arrived at 3 mm position, the pressure value reached 18.77 GPa. It approached to the C–J detonation pressure (around 20.13 GPa) of TNT. In Figure 5(2) for Shot No.2, the input shock pressure was of

Table 3. The shock velocity (U_s) and particle velocity (U_p) of pressed TNT from molecular simulation.

Shock velocity (U_s, mm/μs)	Particle velocity (U_p, mm/μs)
3	0.51
4	0.90
5	1.49
6	2.06

$U_s = 2.15 + 1.89U_p$ (by linear fitting).

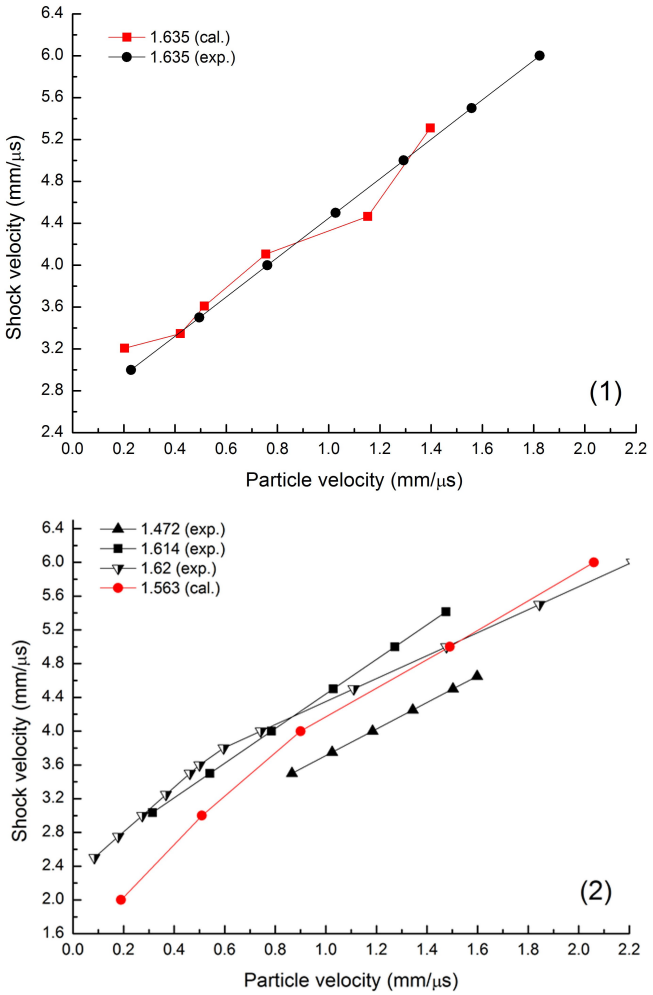

Figure 4. Shock velocity versus particle velocity of TNTs; red line is the calculated values and black line is the experimental values; (1) for 1.635 g cm^{-3} TNT; (2) for TNT with densities of 1.472, 1.614, 1.62 and 1.563 g cm^{-3}.

6.13 GPa, and the ensuing development of pressure was obviously slow compared to the case in Shot No.1. Furthermore, for Shot No.2, it had been found that several yellow explosive grains remained on the bottom witness plate in the experimental test, only leaving a small dent on the plate. Such result indicated that the input pressure of 6.13 GPa was not strong enough to cause a shock to detonation transition in this pressed TNT.

4 Conclusion

In this study, the shock-initiation characteristics of a pressed TNT were investigated by means of both gap experiment and numerical simulation. The pressure-time curves and run distance to detonation data indicated that the pressed TNT behaved much faster reaction rate than that of casted TNT under same shock loading condition. This phenomenon was due that the pressed TNT may possessed more tiny defects inside the sample than ordinary casted TNT. In addition, an Ignition and Growth model of the pressed TNT was accurately parameterized by using the pressure histories from gap experiments, JWL equations of states for unreacted explosive and detonation products. Based on this model the calculated pressure growth histories at different positions could well reproduce the measured values. The determined ignition and growth model would be expected to put in use in subsequent simulation analysis with complex geometrical scenarios.

Supplementary Materials

The Supplementary Materials provided the detailed experiments setups, molecular dynamic method, equation of states calculation and numerical modelling procedures.

Table 4. The JWL equation parameters for unreacted explosive and detonation product.

name	A (GPa)	B (GPa)	R_1	R_2	ω	Cv (J g^{-1} K^{-1})
unreacted explosive	201439.91	−2.18	14.20	1.00	0.89	1.61
detonation products	342.80	4.97	4.26	0.93	0.25	0.66

Table 5. The parameters of reaction rate equation.

I (μs^{-1})	a	b	x	c	d
105000	0.188	0.222	4.0	0.667	0.334
y	e	g	z	G_1 (GPa^{-2} μs^{-1})	G_2 (GPa^{-3} μs^{-1})
2.0	0.111	1.0	3.0	0.048	0.00078
F_{igmax}	$F_{slowmax}$	$F_{fastmin}$	ρ_0 (g cm^{-3})	E_0 (J/g)	
0.5	0.5	0.5	1.563	4536.1	

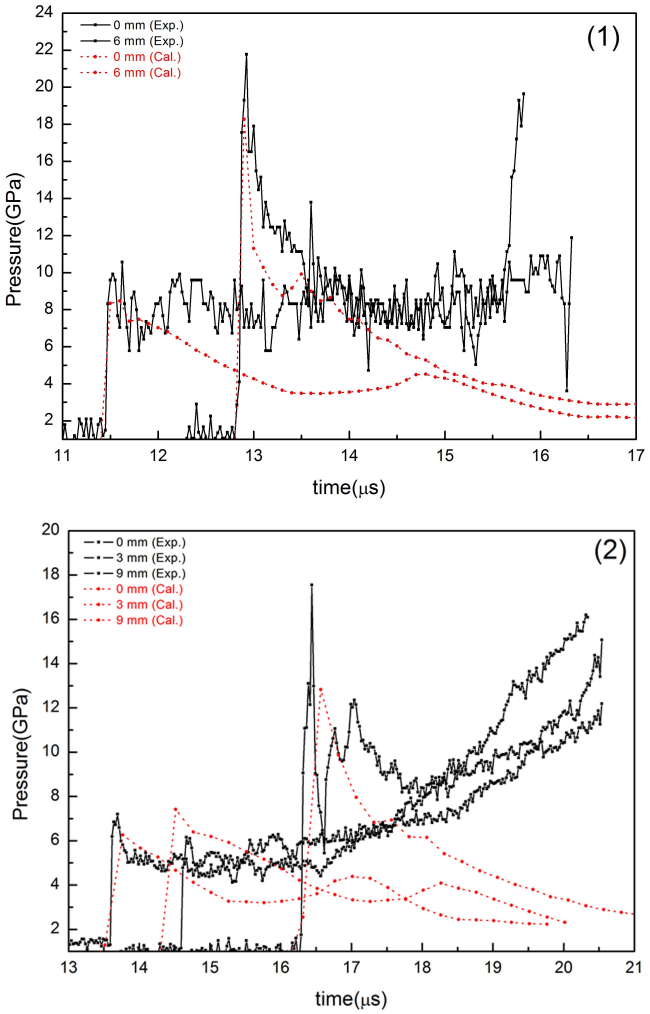

Figure 5. The experimental and calculated pressure histories; (1) for Shot No.1 and (2) for Shot No.2.

Acknowledgements

The authors would like to thank the Fundamental Research Funds for the Central Universities in China.

Data Availability Statement

The data that support the findings of this study are available from the corresponding author upon reasonable request.

References

[1] E. C. Koch, V. Weiser, E. Roth, 2, 4, 6-Trinitrotoluene: a Surprisingly Insensitive Energetic Fuel and Binder in Melt-cast Decoy Flare Compositions, *Angew. Chem. Int. Ed.* **2012**, *51*, 10038. doi: 10.1002/anie.201204808.

[2] E. L. Lee, C. M. Tarver, Phenomenological Model of Shock Initiation in Heterogeneous Explosives, *Phys. Fluids* **1980**, *23*, 2362. doi: 10.1063/1.862940.

[3] G. P. Jiang, S. Huan, Experimental Investigation and Lagrange Method Used for Small Partition Assay, *Explosion and Shock Waves* **2005**, *5*, 90–94.

[4] Y. M. Belinets, A. N. Dremin, Kinetics of Pressed-TNT Decomposition behind a Shock Front, *Combust. Explos. Shock Waves* **1978**, *14*, 361. doi: 10.1007/bf00740505.

[5] G. I. Kanel, Kinetics of the Decomposition of Cast TNT in Shock Waves, *Combust. Explos. Shock Waves* **1978**, *14*, 92. doi: 10.1007/bf00789176.

[6] S. Kubotal, Y. Ogatal, Y. Wadal, K. Katohl, T. Saburil, M. Yoshidal, K. Nagayama, Observation of Shock Initiation Process in Gap Test, *AIP Conf. Proc.* **2006**, *845*, 1085. doi: 10.1063/1.2263511.

[7] P. A. Urtiew, C. M. Tarver, Shock Initiation of Energetic Materials at Different Initial Temperatures (Review), *Combust. Explos. Shock Waves* **2005**, *41*, 766. doi: 10.1007/s10573-005-0085–0.

[8] L. C. Liu, Y. Liu, S. V. Zybin, H. Sun, W. A. Goddard, ReaxFF-lg: Correction of the ReaxFF Reactive Force Field for London Dispersion, with Applications to the Equations of State for Energetic Materials, *J. Phys. Chem. A* **2011**, *115*, 11016. doi: 10.1021/jp201599 t.

[9] E. J. Reed, L. E. Fried, M. R. Manaa, J. D. Joannopoulos, A Method for Tractable Dynamical Studies of Single and Double Shock Compression, *AIP Conf. Proc.* **2004**, *706*, 259. doi: 10.1063/1.1780230.

[10] J. M. Walsh, R. H. Christian, Equation of State of Metals from Shock Wave Measurements, *Phys. Rev.* **1955**, *97*, 1544. doi: 10.1103/PhyRev.97.1544.

[11] M. Sućeska, Calculation of Detonation Parameters by EXPLO5 Computer Program, *Mater. Sci. Forum* **2004**, *465*, 325. doi: 10.4028/www.scientific.net/MSF.465-466.325.

[12] C. M. Tarver, Ignition and growth modelling of LX-17 hockey puck experiments. *Propellants Explos. Pyrotech.* **2005**, *30*,109-112. doi: 10.1002/prep.200400092.

[13] A. W. Campbell, W. C. Davis, J. B. Ramsay, J. R. Travis. Shock Initiation of Solid Explosives, *Phys. Fluids* **1961**, *4*, 511–521. doi: 10.1063/1.1706354.

[14] B. M. Dobratz. LLNL explosives handbook: properties of chemical explosives and explosives and explosive simulants, Lawrence Livermore National Laboratory, California, CA, USA **1985**.

Manuscript received: March 8, 2021
Revised manuscript received: July 26, 2021
Version of record online: September 24, 2021